*Розроблено нову конструкцію повітряного колектора з герметичним і утепленим корпусом та абсорбер з хвилястою поверхнею, що може використовуватися як додатковий нагрівний елемент низькотемпературного джерела теплоти. Встановлено ряд узагальнювальних залежностей для знаходження теплової ефективності колектора, а саме впливу складових теплового балансу колектора на перепад температур потоків теплоносія у колекторі та рівня інсоляції, на теплопродуктивність.*

*Отримані аналітичні залежності для визначення складових теплового балансу колектора, розподілення поля температур вздовж поглинальної панелі, що дало змогу вдосконалити математичну модель процесу теплообміну в розробленому повітряному колекторі. Результати досліджень повітряного колектора дозволили розробити програму чисельного розрахунку температурного поля теплових потоків на ЕОМ.*

*З'ясовано, що застосування хвилястої поглинаючої поверхні абсорбера у повітряному геліоколекторі за малого рівня інсоляції E=377 Вт/м² дає змогу збільшити ККД до η=58,3 %, а при великій енергетичній освітленості у E=1000 Вт/м² до η=63,9 %. Ітераційним розрахунково-кількісних шляхом визначено ефективність роботи колектора, яка становить понад 78–80 %. Це на 10–20 % вище, ніж у пласких колекторів, і на 5–10 % вище ніж у циліндричних вакуумованих колекторів.*

*Отримані результати можна використати під час розробки та вдосконалення технічних засобів сушіння фруктів, для підвищення технологічної та енергетичної ефективності процесу*

*Ключові слова: геліоколектор, повітряна система опалення, абсорбер, тепловий потік, критерій Релея, теплопродуктивність*

# RESULTS OF RESEARCH INTO EFFICIENCY OF A FLAT SOLAR AIR HELIOCOLLECTOR WITH A WAVY ABSORBING SURFACE

**V. Boyarchuk**
PhD, Professor*
E-mail: vim2@ukr.net
**S. Korobka**
PhD, Senior Lecturer*
E-mail: korobkasv@ukr.net
**M. Babych**
PhD*
E-mail: m.babych@ukr.net
**R. Krygul**
PhD*
E-mail: krroma@ukr.net
*Department of Energy
Lviv National Agrarian University
V. Velykoho str., 1, Dublyany, Ukraine, 80381

## 1. Introduction

At present, there are many heliocollectors that are industrially produced. These heliocollectors are used mainly to obtain a low-potential heat carrier because their existing designs do not make it possible to perform heating to higher temperatures, specifically, 50–60 ºC. Flat collectors with efficiency of 50–60 % make up 92 % among the mounted heliocollectors in Europe. A flat air heliocollector (AHC) is a device for collecting solar energy in the visible and infrared range and converting it into heat energy. An absorber is an artificial material, capable of absorption (for example, a corrugated copper sheet coated with black selective paint). The main requirement for the absorbers used in AHC is a high absorbing ability regarding the absorbed component, specifically, solar energy. A valuable quality of absorbers is the ability to regenerate, which makes the technological process cheaper. In addition, the absorbent should be chemically indifferent to the absorbate and chemically resistant (to splitting, oxidation, resinification, etc.), cheap and corrosion-inactive.

The study of performance of AHC is reduced to finding directions to reduce heat losses, increase heating efficiency and intensify heat exchange between the absorber and the heat carrier. It is also important to select the most productive form of surface of absorbing plates that have good energy characteristics. In particular, an increase in heating efficiency, a decrease in heat losses, small consumption of pressure to transfer air masses through the collector do not require additional energy consumption and money costs for the production. In this regard, the subject matter of the research devoted to studying the performance of AHC with the wavy absorption surface is relevant.

## 2. Literature review and problem statement

Paper [1] proposed the structure of an air heliocollector with two absorbers in the form of the plate and jet absorbing surface. It presented the results of the field experimental studies to determine the thermal effectiveness of the heliocollector taking into consideration the mode of motion of the heat carrier and the degree of its heating. However, when calculating the thermal efficiency of the heliocollector, two outgoing flows of heat consumption were not taken into consideration: convective with heat transfer coefficient de-

pending on air velocity, and radiative with the environment at ambient temperature. This does not make it possible to describe the change in the maximum energy illuminance of the horizontal surface of the air collector relative to daily illuminance.

In paper [2], the operation of the developed experimental design of the heliocollector was analyzed and its thermal balance and efficiency were calculated. The main components of energy losses in the environment were determined based on the results of a series of studies of the plant in the summer period in the normal operating mode and in the stagnation mode. However, the constituent magnitudes of temperature ranges and temperature difference between the parallel surfaces, specifically, the back surface of the absorber and the air channel, were not taken into consideration in the study.

The authors of paper [3] described the effectiveness of the combination of roofing material of the building and the solar collector. They established the relationship between the angles of mounting the combined solar collector relative to the air flow arrival and its efficiency. They obtained the dependences between different velocities, directions of the air flow and efficiency of the solar collector and showed how effectiveness of the combined solar collector decreases when it is exposed to the wind effect. The components of coefficients of the heat flow equation associated with thermal resistances were not taken into consideration, specifically, coefficients of convective heat transfer, of radiative (radiant) heat transfer and specific coefficient of thermal conductivity.

In study [4], authors developed a new air collector with the absorber of the wavy type, which operates exclusively on solar energy by the principle of simultaneous ventilation of premises for heating for the subtropical climatic conditions of the city of Ankara (Turkey). Selective coating for the absorbing surface of the absorber was chosen, based on high performance indicators of optical and operating characteristics, specifically, thermal power and energy efficiency of the proposed heliocollector. However, when calculating the heating efficiency of the collector, the heat balance of the glass cover and the absorbing plane (of the absorber) was not taken into consideration. It does not make it possible to calculate the transient modes of the collector operation and heating efficiency.

In paper [5], authors present the method of quality control for solar collectors, which will make it possible to optimize the quality indicators of solar collectors, specifically, the indicators of safety, performance and efficiency and to establish their performance by efficiency coefficient, expressed as an integrated quality indicator. However, the components of the convective and radiative heat exchange of the glass surface were not considered.

The authors of study [6] analyzed the known methods for calculation of air solar collectors. They proposed the method for calculating the system of solar heat supply with solar panels. The authors developed the algorithm for computer calculation of the system of solar heat supply with solar panels taking into consideration the impact of direct and scattered solar radiation on the effectiveness of a solar panel. However, the radiation component of coefficient of heat transfer from the absorbing plate to the glass cover, which is considered during the calculation of long-wave (thermal) radiation, was not taken into consideration.

Paper [7] demonstrates processes of heat exchange in a flat collector of solar energy, which is a part of the plant, designed for heating the premises by hot air. The thermal balances of translucent cover, the heat of the accepting metal plate and the layer of insulation, as well as the overall heat balance of the collector were presented. The results of the calculation of intensity of air heating in the collector of solar energy within the initial period of time at different air flows were shown. It was emphasized that it is necessary to make the final decision on the optimal amount of air that circulates in the plant based on the joint analysis of heat balances of the solar energy collector and the chamber for thermal treatment of water-proof concrete products. However, it was investigated how the temperature of the heat carrier at the outlet from the collector and coefficients of heat flows, associated with thermal resistances, influence heating efficiency of the heliocollector.

The methods for selection and calculation of the air solar collector were developed mainly for the countries with hot climate, for example, for subtropical climatic conditions of Turkey, Iran, Bulgaria, Greece, Croatia, etc. Most of the methods for selection and calculation of thermal engineering characteristics of the air solar collector were implemented using the imitation models during computer simulation. Here, the presented designs of air solar collectors need modification and improvement in order to increase efficiency under conditions of temperate continental climate in Ukraine and decrease capital and operational costs.

Thus, a crucial aspect for making decisions when using air solar collectors in a solar drying chamber is substantiation of its optimal design and technological parameters.

## 3. The aim and objectives of the study

The aim of this research is to improve effectiveness of using solar energy in a solar drying chamber based of the development of a new design of the absorber with the wavy surface for the air solar collector, as well as the improvement of its methods for calculating energy characteristics.

According to the set aim, it was necessary to perform the following tasks:

– to substantiate the need for the development of the new design of the absorber with the wavy surface for the air heliocollector;

– to perform theoretical studies and to obtain analytical dependences for the calculation of energy characteristic of the air heliocollector;

– to carry out the research into the temperature of the heat carrier with the new design of the absorber with the wavy surface for the air heliocollector and to determine its operation effectiveness.

## 4. Materials and methods for substantiation of design and technological parameters of the air solar collector

### 4. 1. Substantiation of design and equipment of the air heliocollector of the solar drying chamber

The measures to improve the efficiency of air collectors as a part of a solar drying chamber are traditionally reduced to decreasing the flows of heat losses at the simultaneous intensification of heat transfer processes. A simple increase in air velocity and its turbulization by additional design elements is usually achieved by an increase in energy consumption to drive a fan, which worsens the economic component of the use of solar energy. A simple increase in the area of the

heat exchange surface by extending the collector or by its additional ribbing has the same result. An alternative option is to increase the area of heat exchange surface by its profiling that simultaneously supports the turbulent air flow mode. Other methods for heat exchange intensification are reduced to creation of zones of pressure drop in channels, large oscillations of the flow or its twisting with the formation of the "tornado"-type vortex [8]. A particular case involves blowing of the flat or profiled surface of the absorbing plane by the vortex flows with the help of the so-called jets [9]. Jets form a narrowly directed air flow, sent to the cylindrical protuberances on the back side of the absorbing plate, where near-surface flows are converted into vortex-like flows. Energy criterion for feasibility of all design solutions is the outrunning increase in heat transfer relative to an increase in energy losses on the respective local resistances.

In the simplest case of air blowing over the illuminated surface of the absorbing plane, the part of heat absorbed by the flow is lost into the environment through the contact with the glass cover. To minimize it, double glazing is used, which reduces the incoming flow of solar energy by 5...10 %, increases material capacity of the collector and degrades its performance characteristics. That is why the best option is the double-chamber (double-slit) design of the collector with the fixed or hardly movable heat insulated layer of the air in the upper slit and turbulent flow of the heat carrier in the lower part (Fig. 1). Both chambers are separated by a profiled metal sheet of the absorbing plane with different types of cover – preferably selectively absorbing at the top and a high coefficient of long-wave radiation at the bottom. This structure of the absorbing plane ensures minimal heat losses through radiation towards the glass and intensification of effective heat transfer due to radiative flow from the back surface to the opposite wall of the lower chamber.
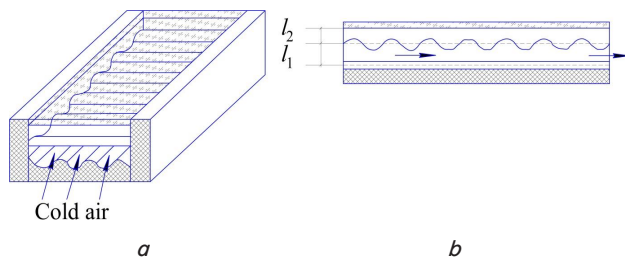


Fig. 1. Schematic cross-section of the air collector:
*a* — projective transverse cut; *b* — longitudinal slit

Additional intensification of heat transfer occurs at the expense of wave-like profiling of the contacting heated surfaces. Such profile is easy to shape from a flat copper or aluminum sheet of the thickness of 02...03 mm without destroying its coating – selectively-absorbing, oxidized or painted. The profiles of the upper profile are oriented across the flow to prevent its sag at a large distance between the lateral walls-supports and the lower one, on the contrary, along the flow. Such cross-orientation of the channel walls provides a turbulent mode of the flow with the elements of vortex-formation at low velocities. The methods for calculation of heat transfer coefficients and assessment of effectiveness of air collectors with air conduits of the similar configuration are based on the known empirical ratios [8–10]. Heat exchange processes of in channels with wave-like walls are by several times more intensive compared with smooth surfaces.

To increase the coefficient of radiation of the back surface of the absorbing panel without worsening the contact heat removal, it is advisable to oxidize it: the blackness degree of oxidized copper is equal to 0.62 and that of soot is 0.95. At the same time, the simplest thing to do is to paint the opposite and side walls of the air channel with the oil paint that is resistant to atmospheric factors, the blackness degree of which is equal to 0.94.

Air collectors are mainly inclined at an angle to the horizon (Fig. 2), which is why the upper edge of the glass cover is always heated up more than the bottom edge with the relevant increase in local heat losses.

To minimize this mechanism of heat losses, it is enough to ventilate the upper slit with a weak laminar flow (draught), through suction by the main flow of the heat carrier at its inlet to the collector or at the outlet. A weak flow makes vertical convective flows curve, prolonging the path to the glass cover, like at an increase in the angle of inclination of the collector [10]. At a weak flow in the ventilation mode, heat losses increase slightly, because low velocities correspond to the laminar mode of flow, and heat across the flow is transferred only by the mechanism of thermal conductivity [11].
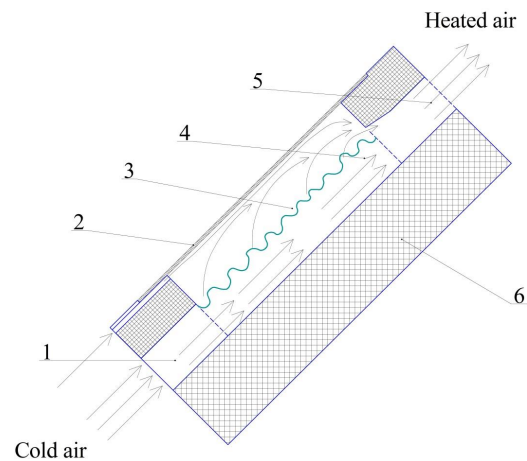


Fig. 2. The scheme of air flows in the inclined collector with sucking the heated air of the upper slit into the heat carrier channel: 1 — inlet channel; 2 — single-layer transparent cover; 3 — absorber; 4 — air duct; 5 — outlet channel; 6 — heat insulation wall

The total coefficient of heat losses of the air collector is generally the effective sum of local coefficients of heat transfer in all directions to the environment. That is why to evaluate it, balance equations of heat flows are constructed separately for the absorbing panel, the glass cover, the flow of the heat carrier and the heat proof case. Here, it is convenient to trace the directions on the circuit of resistance of the electric-thermal analogy, shown in Fig. 3.

Coefficients of the equations of heat flows are associated with thermal resistances by the known ratios:

$$\alpha_c = \frac{1}{R_c} - \text{coefficient of convective heat transfer in W/m}^2\cdot\text{K};$$

$$\alpha_r = \frac{1}{R_r} - \text{coefficient of radiative (radiant) heat transfer in}$$
W/m²·K;

$$\frac{\delta}{\lambda} = \frac{1}{R_\lambda} - \text{specific coefficient of thermal conductivity in}$$
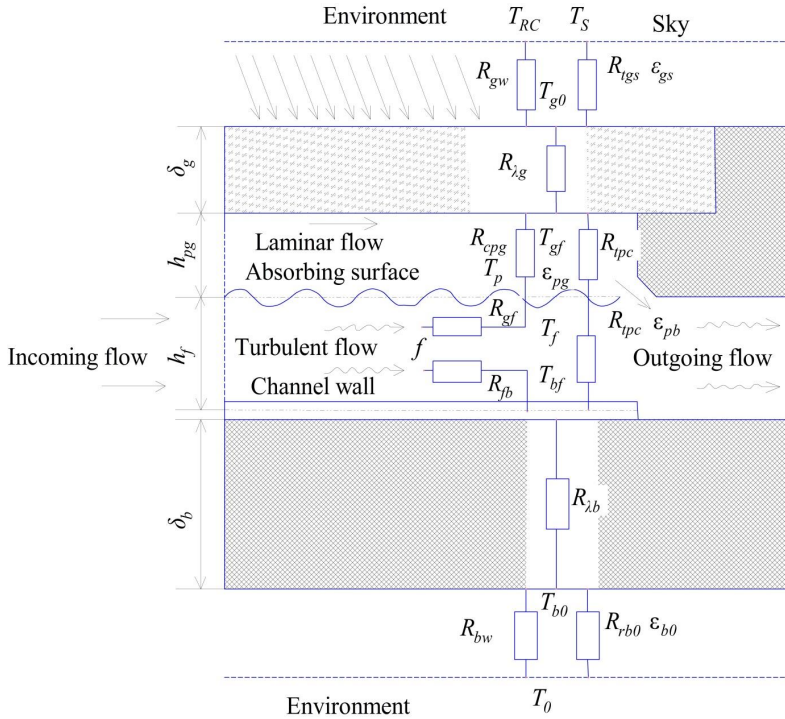W/m²·K.

Fig. 3. Substituting circuit of resistances of flows of heat losses

The indexed magnitudes, shown in Fig. 3, have the following physical sense: $h_{pg}$ is the average height of the slit between the absorbing profiled surface and the glass; $h_f$ is the average height of the slit (channel) of the air flow (heat carrier); $R_{ij}$ is the thermal resistance; $T_a$ is the ambient temperature, K; $\delta$ is the thickness, m; $\varepsilon_{ij}$ is the reduced coefficient of radiative (radiant) heat transfer; $\lambda$ is the coefficient of thermal conductivity, W/m·K; $\alpha_g$=0.03 is the integrated coefficient of absorption of the solar radiation flow by glass, which is estimated by transmission curves.

Ordinary and special glass have almost the same absorption coefficients in the visible and ultraviolet region, which account for about half of the entire energy of the solar spectrum. The noticeable difference of coefficients in the infrared region does not give great preference to special glass. Assessing a decrease in the energy contribution with the wavelength by the tables of the spectrum AM 1.5, it is possible to show that in the region of 0.75<λ<2.0 micron, the effectiveness of ordinary glass is approximately by 2 % less, and in the region of 2.0<λ<3.0 micron, only by 1 %. The sun rays in the region of wavelengths of up to λ<2.5 microns transfer 96.8 % of the total capacity of the whole flow, and up to λ<3.5 microns, only by 2 % more – 98.8 %. The difference of the energy flow by 3.2 % during using the ordinary window glass is not lost irrevocably, because during absorption the glass is heated, which reduces the flow of heat losses from the absorbing panel towards the environment due to reducing the temperature difference. According to the research data [12], coefficient of long-wave radiation (emission) of ordinary glass is equal to $\varepsilon_g$=0.84. Besides, the cumulative coefficient of transmittance of solar energy of polycarbonate is 10 % lower than that of glass [12], it is 3.2 % lower in the ultraviolet range and 7.1 % lower in the visible region, whereas it differs insignificantly in the infrared range. The glass of the width $W$=1.3 m, the length $L$=1.7 m and the thickness δ=0.05 m was used in the design.

The absorbing panel is made of a copper sheet of the thickness of 0.5 mm with the corrugated wavy surface of the radius of rounding of 3 cm. From the illuminated side, its surface is oxidized by the method of chemical etching in soda solution, due to which it is performed and gains selective properties with coefficient of absorption of the order of α=0.9 and the blackness degree ε=0.16 [12]. Another option is covering with soot (α=0.94), including its back surface to increase the coefficient of radiation heat transfer (emission) with ε=0.94 toward the back wall. Its profiled surface is also covered with soot, due to which it almost completely absorbs the radiation of the panel, is heated and gives away extra heat to the air flow. The width and the length of the back wall is accepted the same as those of the glass cover.

## 4. 2. Substantiation of thermo-technical characteristics of the air heliocollector

The main characteristics of the solar collector include useful specific (per unit of area) heating efficiency $q_u$ and its effectiveness, quantitatively assessed by efficiency η, is described by such classical equations of the balance of energy flows, respectively:

$$q_u = F_R\left[\eta_0 E - U_L(t_{cp}-t_a)\right]; \tag{1}$$

$$\eta = F_R\left(\eta_0 - U_L\frac{t_{cp}-t_a}{E}\right). \tag{2}$$

Where the multiplier

$$F_R = \frac{G_m c_p}{U_L}\left(1 - e^{-\frac{F'U_L}{G_m c_p}}\right) \tag{3}$$

is called by the general coefficient of thermal removal (consumption) of the solar collector; $E$ is the energy illuminance of the absorbing surface; $U_L$ is the general coefficient of thermal losses of the collector into the environment; $T_f$=$(T_o - T_i)/2$ is the average temperature of the heat carrier along the collector; $T_a$ is the ambient temperature; $F'$ is the coefficient of effectiveness of the absorbing panel; $G_m$ is the mass consumption of the heat carrier (air); $c_p$ is the specific thermal capacity of the heat carrier (air) at constant pressure [1–3].

The temperature of the incoming flow in air collectors is usually equal to the ambient temperature $T_i$=$T_a$. In flow-through air collectors, the temperature of the absorbing panel increases along the flow of the heat carrier, while it remains constant across the flow. If in this case the contact with the heat carrier flow comes directly with the heated surface or back side, the corresponding structure is called a slit collector [4]. For it, the coefficient of effectiveness of the absorbing panel is equal to the ratio of useful heat flow to the incoming flow $\eta_0 E$. The latter in any collector is equal to the sum of two flows – the useful flow and the heat losses flow:

$$F' = \frac{q_u}{q_u + q_{hl}}. \tag{4}$$

Coefficient of effectiveness of the absorbing panel is close to unity ($F'$→1) at the very large mass consumption of the

heat carrier ($G_m{\rightarrow}\infty$). At the same time, at the fixed heat carrier ($G_m{\rightarrow}0$ i $F'{\rightarrow}0$), the temperature of the outgoing flow increases to a maximum (equilibrium) value.

Collectors of the solar heat supply systems typically operate in the modes of optimum heating efficiency at low increments in temperature. At the same time, in the ventilation systems or drying chambers, much attention is paid to the temperature mode of the outgoing flow. The original parameters of solar collectors are calculated by passport characteristics, which first of all include optical efficiency $\eta_0$ and product of coefficient of efficiency of absorbing panel and total coefficient ($F'{\cdot}U_L$).

The main function of the collector of the solar drying chamber is to increase the air flow as a drying agent by means of raising its temperature within the measures assigned by the technological process. At the initial stage with intense natural moisture release, it is generally recommended to apply a low-temperature mode with increased multiplicity of the air exchange in the drying chamber. At the later stages, it is necessary to stimulate the process of moisture release additionally through slowing down the natural diffusion processes inside the dried material. Accordingly, it is required to transfer the collector to the mode with elevated temperature of the heat carrier and its lower consumption with a corresponding decrease in heating capacity and efficiency.

### 4. 3. Substantiation of the methods for calculation of parameters of the air collector

Effectiveness of an air collector as a part of a drying chamber is assessed by two main parameters – thermal conductivity and output temperature of the heat carrier flow. These parameters are functionally interrelated with the kinetic and thermo-physical parameters of many independent input magnitudes, the system of equations of balance of heat flows at determining elements of the structure.

The thermal balance of the glass cover consists of three incoming flows and two outgoing flows. The incoming flows include the absorbed fraction of incident solar energy flow $\alpha_g E$ and the flow of radiation from the heated panel $\alpha_{rpg}(T_p{-}T_g)$, as well as convective $\alpha_{cpg}(T_p{-}T_g)$ flow through the air layer $h_{pg}$. At the same time, two outgoing flows of thermal losses – convective, with heat transfer coefficient, dependent only on wind velocity $V_w$ ($\alpha_w{=}5.7{+}3.8V_w$) and radiative with the environment at temperature $T_a$ and the upper layers of the atmosphere with the temperature of the sky $T_s$. If we neglected absorption in glass, the equation of thermal balance of glass cover can be reduced to the following form:

$$\alpha_g E+\left(\alpha_{cpg}+\alpha_{rpg}\right)\left(T_p-T_g\right)=\left(\alpha_w+\alpha_{rga}\right)\left(T_g-T_a\right). \tag{5}$$

The heat balance of the absorbing panel consists of one incoming (absorbed) flow of solar energy $E\eta_0$ and four outgoing flows. Optical efficiency of the collector $\eta_0$ is equal to the product of coefficients of absorption of glass $\tau$ and absorption of the surface of the receiving panel $\alpha_p$. Convective flow $\alpha_{cpg}(T_p{-}T_g)$ and radiative flow $\alpha_{rpg}(T_p{-}T_g)$ move towards the glass cover, and from the back side, the convective flow moves to the flow of the heat carrier $\alpha_{cpf}(T_p{-}T_f)$ and the radiative flow moves to the opposite walls of the air channel $\alpha_{rpb}(T_p{-}T_b)$. It is common to consider the temperature of the heat carrier inside the air channel as average between its input and output values $T_f{=}0.5(T_i{+}T_o)$, which, however, it not quite correct. Therefore, the equation of

thermal balance of the absorbing panel can be reduced to the following form:

$$\eta_0 E =\left(\alpha_{cpg}+\alpha_{rpg}\right)\left(T_p-T_g\right)+$$
$$+\alpha_{cpf}\left(T_p-T_f\right)+\alpha_{rpb}\left(T_p-T_b\right). \tag{6}$$

The absorbing panel transmits thermal capacity of the air flow $\alpha_{cpf}(T_p{-}T_f)$, the main part of which transfers to the useful heat flow $G_m{\cdot}c_p{\cdot}(T_i{-}T_o)$, and its smaller part – the flow of heat losses – to the walls of the air channel $\alpha_{cfb}(T_f{-}T_b)$. Therefore, the balance of powers of the heat carrier flow is described by the following equation:

$$\alpha_{cpf}\left(T_p-T_f\right)=G_m c_p\left(T_{\text{вих}}-T_{\text{вх}}\right)+\alpha_{cfb}\left(T_f-T_b\right). \tag{7}$$

Finally, two flows of heat losses towards the walls of the air channel from the absorbing panel $\alpha_{rpb}(T_p{-}T_b)$ and from the heat carrier $\alpha_{cfb}(T_f{-}T_b)$ inside the thermal insulation are united into a single flow towards the environment. Given that the temperature of the external surface of thermal insulation $T_{ba}$ and the environment differ insignificantly, provided that $T_{ba}{\approx}T_a$, the flow of heat losses in the environment through the casing of the collector is equal to $(\lambda/\delta){\cdot}(T_b{-}T_a)$. In other words, both parallel resistances of the external part of the chain of heat losses ($R_{rba}$; $R_w$)$\rightarrow 0$ and the balance of the flows on the internal side of the channel of the heat carrier is reduced to the following equation:

$$\alpha_{pb}\left(T_p-T_b\right)+\alpha_{cfb}\left(T_f-T_b\right)=\frac{\lambda}{\delta}\left(T_b-T_a\right). \tag{8}$$

On condition of equality $T_i{=}T_a$, $\alpha_{cpf}{=}\alpha_{cfb}$, the following expressions are obtained for the correspondent temperatures by elementary transformations:

$$T_g=\frac{\alpha_g E+\left(\alpha_{cpg}+\alpha_{rpg}\right)T_p+\left(\alpha_w+\alpha_{rgs}\right)T_a}{\alpha_{cpg}+\alpha_{rpg}+\alpha_w+\alpha_{rgs}}, \tag{9}$$

$$T_b=\frac{\dfrac{\lambda}{\delta}T_a+\alpha_{rpb}T_p+\alpha_{cpf}T_f}{\dfrac{\lambda}{\delta}+\alpha_{rpb}+\alpha_{cpf}}, \tag{10}$$

$$T_f=\frac{\alpha_{cpf}\left(T_p+T_b\right)+2G_m c_p T_a}{2\alpha_{cpf}+2G_m c_p}, \tag{11}$$

$$T_o=2T_f-T_a. \tag{12}$$

In this case

$$T_p=\frac{\eta_0 E+\left(\alpha_{cpg}+\alpha_{rpg}\right)T_g+\alpha_{rpb}T_b+\alpha_{cpf}T_f}{\alpha_{cpg}+\alpha_{rpg}+\alpha_{rpb}+\alpha_{cpf}}. \tag{13}$$

All magnitudes of compound equations are interconnected and are the independent input parameters of the process of energy transformations, which is why it is possible to determine them only by numerical methods with the use of the methods for successive approximations (iterations). The number of iterative steps decreases during the selection of the initial values close to the original, selected according to the known regularities or the results of previous studies, including those listed in the literature [8].

The classic equation of the solar fluid collector is not used in the numerical modeling of heat flows either, because of the complicated dependence of coefficient of general heat losses $U_L$ on the design of the air channel and the air flow modes. It is not appropriate to use the known ratios to evaluate the flows of the upper heat losses (through glass) in the environment, which is a result of generalization of the typical characteristics of fluid collectors [11]. As noted in [12], such ratios in many cases allow considerable deviations from the values, established experimentally. Therefore, the ratios, for which there are no warnings in the specialized literature, are subsequently used to assess coefficients of heat transfer in the air layers.

Approximation formulas for kinematic viscosity and thermal conductivity in the temperature interval of the Celsius scale from $t=[0; 100 \text{ °C}]$ were obtained with the following coefficients:

$$\nu = (13,53 + 0,0904t + 0,0001t^2) \times 10^{-6} \text{ m}^2 / \text{s}, \qquad (14)$$

$$a = (18,8 + 0,128t + 0,0002t^2) \times 10^{-6} \text{ m}^2 / \text{s}. \qquad (15)$$

At the same time, the temperature dependence of coefficient of thermal conductivity of the air is less complex and is easier to approximate by linear dependence

$$\lambda = (2,44 + 0,0077t) \times 10^{-2} \frac{\text{W}}{\text{m} \cdot \text{K}}. \qquad (16)$$

It is obvious that coefficients of these equations will be different in the Kelvin scale.

Coefficient of convective heat transfer in the inclined slit of the height $h_{pg}$ from the absorbing panel to the parallel glass surface of consumptions $\alpha_{cpg}$ is estimated by the typical ratios, presented, for example, in [13], for typical and special conditions of heat exchange:

$$\alpha_{cpg} = \frac{\lambda Nu}{h_{pg}}, \qquad (17)$$

where $\alpha$ is the coefficient of heat transfer in W/m²·K, $\lambda$ is the coefficient of thermal conductivity of the air in the temperature range in W/m·K.

In the angular interval of the inclinations of parallel plates (collector) to the horizon plane $\beta$ from 0 to 75°, Nusselt number is calculated through Rayleigh number by the following ratio:

$$Nu = 1 + 1,44 \left[ 1 - \frac{1708(\sin 1,8\beta)^{1,6}}{Ra \cdot \cos\beta} \right] \left[ 1 - \frac{1708}{Ra \cdot \cos\beta} \right] +$$
$$+ \left[ \left( \frac{Ra \cdot \cos\beta}{5830} \right)^{1/3} - 1 \right]^{+}. \qquad (18)$$

Sign (+) instead of power of the last term means that only the positive value of the expression in square brackets is accepted, whereas at the negative value, it is considered to be equal to zero. In the particular case $\beta=45°$, expression (18) is simplified to form (19):

$$Nu = 1,44 \left( 1 - \frac{2368}{Ra} \right) \cdot \left( 1 - \frac{2415}{Ra} \right) + 0,0495(Ra)^{0,3333}. \qquad (19)$$

Here the optimal angular intervals of inclinations of parallel plates to the plane of the horizon $\beta$ are determined by the maximum solar energy that arrives onto its surface during daylight hours. That is why instead of cumbersome calculations for each month of the season of the collector operation, it is appropriate to use the results of the calculations, presented on the NASA site [14].

Rayleigh criterion, in its turn, is calculated from the following formula

$$Ra = \frac{g\beta_V \Delta T h_{pg}^3}{\nu a}, \qquad (20)$$

where $\nu$ is the kinematic viscosity of the air that is average in the temperature range, m²/s; $a$ is the thermal conductivity of the air that is average in the temperature range, m²/s; g=9.81 m/s² is the free fall acceleration; $\beta_V=1/T_{cp}$ is the coefficient of the volume expansion of the air; $T$ is the absolute temperature, K; $\Delta T$ is the temperature range or the difference of temperatures between the parallel surfaces.

The radiative component of coefficient of heat transfer from the absorbing panel to the glass cover is calculated from the formula for parallel plates:

$$\alpha_{rpg} = \frac{1}{R_{rpg}} = \varepsilon_{pg}\sigma\left(T_p^2 + T_g^2\right)\left(T_p + T_g\right), \qquad (21)$$

where $\sigma=5.67 \cdot 10^{-8}$ W/m²·K⁴ is the Stefan-Boltzmann constant.

Full coefficient of heat transfer to the inside surface of the glass is equal to:

$$\alpha_{pg} = \alpha_{cpg} + \alpha_{rpg} = Nu\frac{\lambda}{h_{pg}} + \varepsilon_{pg}\sigma\left(T_p^2 + T_g^2\right)\left(T_p + T_g\right). \qquad (22)$$

Thermal equilibrium of the glass cover is determined by the balance of two incoming flows, examined above, and two outgoing flows of heat losses into the environment. The convective component of this flow is independent on temperature and is determined by the average wind velocity and the collector orientation relative to its direction. Collectors of drying chambers are usually located slightly above the surface of the ground, where wind velocity $w$ is less than the average, determined at ten-meter height of the weather vane and its direction changes randomly under the influence of local obstacles. To do this, we will use the ratio:

$$\alpha_w = 5,7 + 3,8w. \qquad (23)$$

Radiative heat losses from the external surface of the glass into the environment are spatially divided into two components – to the nearest surroundings (environment) with temperature $T_a$ and the upper cooler layers of the atmosphere with the temperature of the sky $T_s$, which is common to evaluate by the following empirical ratio:

$$T_s = 0,0552T_a^{1,5}. \qquad (24)$$

At an arbitrary angle of inclination $\beta$, the full flow of the radiative heat exchange is equal to the sum of the flows from the closed and open parts of the sky, which can be presented with the following expression

$$q_{r\infty} = q_{ra} + q_{rs} = \alpha_{rga}\frac{\beta}{180}\left(T_g - T_a\right) + \alpha_{rgs}\left(1 - \frac{\beta}{180}\right)\left(T_g - T_s\right). \qquad (25)$$

Therefore, the expression for effective coefficient of radiative heat losses from the glass into the environment $\alpha_{r\infty}$ is

obtained by dividing both parts (24) into the difference in temperature in each of the terms:

$$\alpha_{r\infty} = \frac{q_{r\infty}}{T_g - T_a} = \alpha_{rga}\frac{\beta}{180} + \alpha_{rgs}\left(1 - \frac{\beta}{180}\right). \tag{26}$$

To minimize the volume of calculations, partial heat transfer coefficients are written down in the classical form of

$$\alpha_{rga} = \varepsilon_g \sigma \frac{T_g^4 - T_a^4}{T_g - T_a} \text{ and } \alpha_{rgs} = \varepsilon_g \sigma \frac{T_g^4 - T_s^4}{T_g - T_s}. \tag{27}$$

So, the full coefficient of heat losses from the glass into the environment is equal to

$$\alpha_{g\infty} = \alpha_w + \alpha_{rga} =$$
$$= \alpha_w + \varepsilon_g \sigma \frac{T_g^4 - T_a^4}{T_g - T_a}\frac{\beta}{180} + \varepsilon_g \sigma \frac{T_g^4 - T_s^4}{T_g - T_s}\left(1 - \frac{\beta}{180}\right). \tag{28}$$

After ordering and reducing to the constant angle of inclination $\beta=45°$

$$\alpha_{g\infty} = \alpha_w + \varepsilon_g \sigma \left[ 0,25\frac{T_g^4 - T_a^4}{T_g - T_a} + 0,75\frac{T_g^4 - T_s^4}{T_g - T_s} \right]. \tag{29}$$

The flows of heat transfer of the back surface of the absorbing panel are transferred directly to the heat carrier and by radiation to the opposite and lateral sides of the air channel. Coefficient of convective heat transfer of the wavy-profiled surface of the channel of turbulent heat carrier flow is estimated by the known ratios [8]:

$$\alpha_{cpf} = \frac{\lambda Nu}{D_h}; \tag{30}$$

$$Nu_{pf} = 0,0743\,\mathrm{Re}^{0,76}; \tag{31}$$

$$\mathrm{Re}_f = \frac{\overline{\upsilon}D_h}{\nu_f}, \tag{32}$$

where $\overline{\upsilon}$ is the average velocity of the air flow in m/s; $\nu$ is the kinematic viscosity of the air in m²/s.

Hydraulic diameter of the air channel of height $h_f$ and width $W$ is determined from

$$D_h = \frac{2Wh_f}{W + h_f}. \tag{33}$$

Radiative component of heat transfer from the back side of the absorbing panel to the opposite wall of the channel is estimated by the same ratio as for the upper slit (18). If we neglect radiative features of the irradiated area due to profiling and by an additional contribution of the side walls:

$$\alpha_{rpb} = \frac{1}{R_{rpb}} = \varepsilon_{pb}\sigma\left(T_p^2 + T_b^2\right)\left(T_p + T_b\right). \tag{34}$$

The coefficient of heat transfer from the turbulent flow of the heat carrier to the profiled walls of the air channel is equal to that for heat transfer from the absorbing panel into the flow:

$$\alpha_{cfb} = \alpha_{cpf}. \tag{35}$$

The values of temperatures and coefficients of heat transfer, derived as a result of the iteration process, correspond only to a specific set of input parameters and the process must be repeated anew for each new set. For example, the results presented in paper [8] make it possible to predict the magnitude and the direction of a change of the respective operation characteristics of the collector, depending on a change of one of the input parameters, which is important for theoretical constructions. At the same time, in the case of practical installations, it is more appropriate to use the calculated coefficients of heat transfer to assess the parameters of the classical equation of the collector – coefficients of total heat losses $U_L$ and of effectiveness of absorbing panel $F$. It is more convenient to assess the performance characteristics of the collector at a different ratio of input values.

Full coefficient of heat losses is equal to the sum of two components

$$U_L = U_t + U_b. \tag{36}$$

where $U_t$ and $U_b$ are the coefficients of the upper (through the glass) and lower (through the walls of the casing) losses of the collector. From the substituting circuit in Fig. 3, coefficient of the upper heat losses is determined from the following ratio of coefficients of heat transfer:

$$U_t = \frac{1}{\dfrac{1}{\alpha_{cpg} + \alpha_{rpg}} + \dfrac{1}{\alpha_w + \alpha_{rg\infty}} + \dfrac{\delta_g}{\lambda_g}}. \tag{37}$$

The flow of the lower heat losses occurs through the back wall by the area, which is equal to the area of the absorbing panel, which is accepted as equal to unity, and two side walls of the air channel having the area $2WLh_f$. The contribution of an increase of the heat scattering surface over the unit area of the absorbing panel can be assessed by the multiplier:

$$\frac{1 + 2WLh_f}{WL}. \tag{38}$$

The total flow of heat losses through them is equal to the sum of partial:

$$q_i = q_b + q_e = \frac{\lambda_i}{\delta_i} \cdot \frac{1 + 2WLh_f}{WL}\left(T_b - T_a\right). \tag{39}$$

Effective thermal resistance of this area of the flow of heat losses will be:

$$R_i = \left(\frac{\lambda_i}{\delta_i} \cdot \frac{1 + 2WLh_f}{WL}\right)^{-1} = \frac{\delta_i}{\lambda_i} \cdot \frac{WL}{1 + 2WLh_f}. \tag{40}$$

Therefore, total resistance $R_b$, coefficient of heat transfer of the lower heat losses $\alpha_{pf}$ and coefficient of lower heat losses are described by the following expressions, respectively:

$$R_b = R_{pf} + R = \left(\frac{1}{\alpha_{cpf}} + \frac{1}{\alpha_{rpf}}\right)^{-1} + \frac{\delta_i}{\lambda_i} \cdot \frac{WL}{1 + 2WLh_f}. \tag{41}$$

$$U_b = \frac{1}{R_b} = \left[\left(\frac{1}{\alpha_{cpf}} + \frac{1}{\alpha_{rpf}}\right)^{-1} + \frac{\delta_i}{\lambda_i} \cdot \frac{WL}{1 + 2WLh_f}\right]^{-1}. \tag{42}$$

Another expression to estimate coefficient of heat losses through casing $U_b$ can be obtained if we compare two expressions for useful heat flow. In particular, in accordance with the equation of the collector [7]:

$$q'_p = \eta_{i0} E - U_L \left( T - T \right). \tag{43}$$

Convective and radiative flows to the walls of the channel are eventually assimilated by the heat carrier. In this case, effective coefficient of heat transfer from the absorbing surface to the heat carrier $\alpha_{pf}$ is simultaneously equal to coefficient of heat transfer $\alpha_h$ and the following ratios are true:

$$q'_u = \frac{T_p - T_f}{1/\alpha_{pf}} = \frac{T_p - T_f}{1/\alpha_h}. \tag{44}$$

Comparing (40) and (41) to exclude the temperature of the absorbing surface, we will obtain the classical equation of the solar collector:

$$q'_u = \frac{\eta_0 E - U_L \left( T_f - T_a \right)}{1 + U_L/\alpha_h} = F'\left[ \eta_0 E - U_L \left( T_f - T_a \right) \right], \tag{45}$$

where

$$F' = \left( 1 + U_L/\alpha_h \right)^{-1} = \frac{\alpha_h}{\alpha_h + U_L}. \tag{46}$$

The last equation is similar to the expression presented in [1] for the air collector with the lower channel of heat carrier without regard to the impact of its side walls on the flow of heat losses:

$$F' = \left[ 1 + \frac{U_L}{\alpha_{cpf} + \left( 1/\alpha_{cpf} + 1/\alpha_{rpb} \right)^{-1}} \right]^{-1}. \tag{47}$$

At the assigned values of input magnitudes, separate intermediate results remain constant throughout the whole procedure of the approximated calculation. That is why to simplify calculations, Table 1 shows previously calculated values that are subsequently considered constant input magnitudes.

Reduced blackness degree (coefficient of radiative heat transfer) $\varepsilon_r$ was calculated from the well-known ratio for parallel planes:

$$\varepsilon_r = \varepsilon_{12} = \frac{1}{\left( 1/\varepsilon_1 + 1/\varepsilon_2 \right) - 1}.$$

In the case of manual calculation, it is appropriate to bring down initial and intermediate values of all magnitudes in accordingly formed tables. In particular, initial values of temperatures are presented in zero line.

Thus, the obtained analytic equations make it possible to calculate the Nusselt (19) and Rayleigh (20) criteria and to estimate heat losses of the solar collector (45).

## 5. Results of iterative calculation of design and technological parameters of the air heliocollector

Field tests of the air solar collector were carried out at the private farm PF "Zoria", located in the town of Korets, Rivne oblast (Ukraine), in the spring-summer period from May 15 to October 25, 2018 [13]. During specification of the standard modes of solar illuminance and typical (seasonal) weather conditions, the results of weather monitoring of the Korets first-grade meteorological station of Rivne oblast (Ukraine) were used.

In the period of testing the air heliocollector from 15.05.2018 to 25.10.2018 in the town of Korets, Rivne oblast (Ukraine), the weather was clear, without precipitation. The degree of atmosphere transparency fluctuated within the range from 0.72 to 0.86. The flow of air masses (wind) ranged between 1.3 m/s up to 2.8 m/s.

The average daily physical parameters of the environment during the period of the research were as follows:

1. Air temperature $t_a$ – 12...32 ºC.
2. Relative air humidity $\varphi_a$ – 12...84.5 %.
3. Energy illuminance $E$ – 100...988 W/m² for the area of the absorbing surface $S_{as}$=1.3 m².
4. Atmospheric pressure of air masses ranged within 720–730 mm Hg.
5. Thermal-technical parameters of the heat carrier (air), which arrived at the outlet channel, were: day time temperature (from 8:00 to 2:00) $t_o$ – 15...71 °C, night time temperature (from 22:00 to 7:00) $t_o$ – 50...14 °C.
6. Velocity of heat carrier (air) circulation $v_o$ – 1...3 m/s.
7. Relative humidity of the heat carrier (air) $\varphi_o$ – 10.8...82.3 %.

In the period of the experimental research, the average value of energy illuminance was within $E$ – 100...988 W/m². When using a flat mirror concentrator, the maximum (1,345.5 W/m²) was recorded on May 16 at 13:00.

During the quantitative-calculation experiments concerning the analysis of the operation of the air solar collector, the numeric values of the thermo-technical characteristics, summarized in Table 1, were found and the technique of step-by-step iteration of the calculation of the air collector was presented.

Table 1

Results of step-by-step calculation of temperatures and heat transfer coefficients

| No. | $\bar{T}_{pg}$ | $\beta_V$ | $v_a$ | Ra | $\alpha_{cpg}$ | $\alpha_{g\infty}$ | $\lambda_f$ | Re$_f$ | $\alpha_{cpf}$ | $T_p$ | $T_f$ |
|---|---|---|---|---|---|---|---|---|---|---|---|
| | $\Delta T_{pg}$ | $\lambda_a$ | $a_a$ | Nu | $\alpha_{rpg}$ | | $v_f$ | Nu$_f$ | $\alpha_{rpb}$ | $T_g$ | $T_b$ |
| 1 | 2 | 3 | 4 | 5 | 6 | 7 | 8 | 9 | 10 | 11 | 12 |
| 0 | $T_p$=60 ºC=333 K; $T_g$=30 ºC=303 K; $T_b$=25 ºC=298 K; $T_f$=25 ºC=298 K; $T_o$=30 ºC=303 K | | | | | | | | | | |
| 1 | 45,318 | 0.0031 | 17.8 | 55,355 | 2.98 | 18.1 | 0.0263 | 4,921 | 16.03 | 48.58 321.58 | 27.68 300.68 |
| | 30 | 0.0279 | 25.0 | 3.20 | 5.65 | | 15.85 | 47.53 | 5.85 | 34.60 307.60 | 35.48 308.48 |

Continuation of Table 1

| 1 | 2 | 3 | 4 | 5 | 6 | 7 | 8 | 9 | 10 | 11 | 12 |
|---|---|---|---|---|---|---|---|---|---|---|---|
| | $T_p$=48.58 °C=321.58 K; $T_g$=34.60 °C=307.60 K; $T_f$=27.68 °C=300.68 K; $T_b$=35.48 °C=308.48 K; $T_o$=35.36 °C=308.36 K; $|\Delta T_o|$=5.36° | | | | | | | | | | |
| 2 | 41.59 314.59 | 0.00318 | 17.46 | 27,561 | 2.48 | 18.17 | 0.0265 | 4845 | 15.95 | 53.53 326.53 | 25.09 298.09 |
| | 13.98 | 0.02760 | 24.47 | 2.70 | 5.65 | | 16.10 | 46.95 | 6.31 | 30.38 303.38 | 32.69 305.69 |
| | $T_p$=53.53 °C=326.53 K; $T_g$=30.38 °C=303.38 K; $T_f$=25,09 °C=298.09 K; $T_b$=32.69 °C=305.69 K; $T_o$=30.18 °C=303.18 K; $|\Delta T_o|$=5.18° | | | | | | | | | | |
| 3 | 41.96 314.96 | 0,00318 | 17,50 | 45,441 | 2.82 | 18.06 | 0.0263 | 4,918 | 16.02 | 50.12 323.12 | 24.85 297.85 |
| | 23.15 | 0,02763 | 24.52 | 3.06 | 5.68 | | 15.86 | 47.51 | 6.38 | 32.24 305.24 | 32.37 305.37 |
| | $T_p$=50.12 °C=323,12 K; $T_g$=32.24 °C=305.24 K; $T_f$=24.85 °C=297.85 K; $T_b$=26.58 °C=299.58 K; $T_o$=29.70 °C=302.70 K; $|\Delta T_o|$=0.48 ° | | | | | | | | | | |
| 4 | 41.18 314.18 | 0.00318 | 17.42 | 35,417 | 2.646 | 18.11 | 0.0263 | 4,925 | 16.04 | 49.35 322.35 | 23.86 296.86 |
| | 17,88 | 0,0276 | 24.41 | 2.877 | 5.631 | | 15.838 | 47.56 | 6.383 | 30.96 303.96 | 31.69 304.69 |
| | $T_p$=49.35 °C=322.35 K; $T_g$=30.96 °C=303.96 K; $T_f$=23.86 °C=296.86 K; $T_b$=31.69 °C=304.69 K; $T_o$=27.72 °C=300.72 K; $|\Delta T_o|$=1.98 ° | | | | | | | | | | |
| 5 | 40.16 313.16 | 0.00319 | 17.32 | 36,980 | 2.666 | 18.08 | 0.0262 | 4,954 | 16.046 | 49.66 322.66 | 24.31 297.31 |
| | 18.39 | 0.0275 | 24.26 | 2.908 | 5.577 | | 15.744 | 47.77 | 6.228 | 30.71 303.71 | 30.66 303.66 |
| | $T_p$=49.66 °C=322.66 K; $T_g$=30.71 °C=303.71 K; $T_f$=24.31 °C=297.31 K; $T_b$=30.66 °C= 303.66 K; $T_o$=28.62 °C= 301.62 K; $|\Delta T_o|$=0.9° | | | | | | | | | | |
| 6 | 40.19 313.19 | 0.00319 | 17.32 | 38,090 | 2.686 | 18.07 | 0.0263 | 4,941 | 16.073 | 47.33 320.33 | 24.24 297.24 |
| | 18.95 | 0.0275 | 24.27 | 2.930 | 5.579 | | 15.787 | 47.67 | 6.205 | 30.83 303.83 | 29.79 302.79 |
| | $T_p$=47.33 °C=320.33 K; $T_g$=30.83 °C=303.83 K; $T_f$=24.24 °C=297.24 K; $T_b$=29.79 °C=302.79 K; $T_o$=28.48 °C=301.48 K; $|\Delta T_o|$=0.14° | | | | | | | | | | |
| 7 | 39.08 312.08 | 0.00320 | 17.216 | 33,696 | 2.595 | 18.073 | 0.0263 | 4,943 | 16.08 | 49.56 322.56 | 23.91 296.91 |
| 8 | 16.5 | 0.0274 | 24.108 | 2.841 | 5.519 | | 15.780 | 47.689 | 6.109 | 29.92 302.92 | 30.28 303.28 |
| | $T_p$=49.56 °C=322.56 K; $T_g$=29.92 °C=302.92 K; $T_f$=23.91 °C=296.91 K; $T_b$=30.28 °C=303.28 K; $T_o$=27.82 °C=300.82 K; $|\Delta T_o|$=0.66 ° | | | | | | | | | | |

$$\nu = (13,53 + 0,0904t + 0,0001t^2) \times 10^{-6} \ \text{m}^2/\text{s}. \qquad (48)$$

$$a = (18,8 + 0,128t + 0,0002t^2) \times 10^{-6} \ \text{m}^2/\text{s}. \qquad (49)$$

$$\lambda = (2,44 + 0,0077t) \times 10^{-2} \ \text{W}/\text{m} \cdot \text{K}. \qquad (50)$$

*Based on the results of step-by-step calculation of the air collector.*

Table 2

Input primary constants and conditionally constant magnitudes

| No. by order | Magnitude | | No. by order | Magnitude | | No. by order | Magnitude | |
|---|---|---|---|---|---|---|---|---|
| | Symbol | Value | | Symbol | Value | | Symbol | Value |
| 1 | $\tau$ | 0.09 | 6 | $\varepsilon_p$ | 0.94 | 11 | $h_f$ | 0.04 m |
| 2 | $\alpha$ | 0.94 | 7 | $\varepsilon_g$ | 0.84 | 12 | $\lambda_g$ | 1.0 W/m·K |
| 3 | $\sigma$ | 5.67·10⁻⁸ W/m²·K⁴ | 8 | $\varepsilon_b$ | 0.94 | 13 | $\delta_g$ | 0.005 m |
| 4 | $g$ | 9.81 m/s² | 9 | $\alpha_b$ | 0.94 | 14 | $\lambda_i$ | 0.04 W/m·K |
| 5 | $c_p$ | 1,005 kJ/kg·K | 10 | $h_{pg}$ | 0.03 m | 15 | $\delta_i$ | 0.06 m |

Table 3

Input secondary (derivatives) conventionally constant magnitudes

| No. by order | Magnitude | | No. by order | Magnitude | | No. by order | Magnitude | |
|---|---|---|---|---|---|---|---|---|
| | Symbol | Value | | Symbol | Value | | Symbol | Value |
| 1 | $\varepsilon_{pg}$ | 0.80 | 4 | $\varepsilon_{pb}$ | 0.89 | 7 | $G_m$ | 0.06 kg/s |
| 2 | $T_s$ | 277 K | 5 | $\bar{\upsilon}$ | 1.0 m/s | 8 | $\eta_0$ | 0.85 |
| 3 | $\alpha_w$ | 13.3 W/m²·K | 6 | $D_h$ | 0.078 | 9 | $\lambda_g$ | 1.0 W/m·K |

*Source data of step-by-step iteration of calculation of the air collector.*

1. Initial values of temperatures: $T_{p0}$; $T_{g0}$; $T_{f\,0}$; $T_{b0}$; $T_{o0}$;

2. To determine: $\overline{T}_{pg}$; $\Delta T_{pg}$; $\beta_V$; $\lambda_n$; $\nu_n$; $a_n$;

3. To determine: Ra; Nu; $\alpha_{cpg}$; $\alpha_{rpg}$; $\alpha_{g\infty}$;

4. To determine: $\lambda_f$; $\nu_f$;

5. To determine: $Re_f$; $Nu_f$; $\alpha_{cpf}$; $\alpha_{rpb}$;

6. To determine original values of temperatures $T_{p1}$; $T_{g1}$; $T_{f1}$; $T_{b1}$; $T_{o1}$;

7. To compare $|T_{o1} - T_{o0}| > 0,1$;

– at $|\Delta|>0{,}1\rightarrow 2$ with new values of temperatures;

– at $|\Delta|<0{,}1\rightarrow$ print $T_p$; $T_g$; $T_f$; $T_b$; $T_o$;

8. To: $U_t$; $U_b$; determine $U_L$; $F'$; $F'\cdot U_L$; $F_R$; $q_u$; $\eta$.

*Step 1 of the iteration of calculation of the air collector*

$T_p$=333 K; $T_g$=303 K; $T_b$=298 K; $T_f$=298 K; $T_o$=303 K.

*Step 2 of the iteration of calculation of the air collector*

$$\overline{T}_{pg} = \frac{T_p + T_g}{2} = \frac{333 + 303}{2} = 318{,}0 \ \text{K},$$

$\Delta T_{pg}$=333–303=30.0,

$$\beta_V = \frac{1}{\overline{T}_{pg}} = \frac{1}{318} = 0{,}00314,$$

$$\lambda = (2{,}44 + 0{,}0077t) \times 10^{-2} = 0{,}0279 \ \text{W/m·K},$$

$$a = \begin{pmatrix} 18{,}8 + 0{,}128(\overline{T}_{pg} - 273) + \\ + 0{,}0002(\overline{T}_{pg} - 273)^2 \end{pmatrix} \times 10^{-6} = 25{,}0 \ \text{m}^2/\text{s},$$

$$\nu = \begin{pmatrix} 13{,}53 + 0{,}0904(\overline{T}_{pg} - 273) + \\ + 0{,}0001(\overline{T}_{pg} - 273)^2 \end{pmatrix} \times 10^{-6} = 17{,}8 \times 10^{-6} \ \text{m}^2/\text{s}.$$

*Step 3 of the iteration of calculation of the air collector*

$$Ra = \frac{g\beta_V \Delta\text{T}_{pg} h_{pg}^3}{\nu a} = \frac{9{,}81 \cdot 30 \cdot 0{,}03^3}{17{,}8 \cdot 25{,}0} \times 10^{12} = 55355,$$

$$Nu = 1{,}44\left(1 - \frac{2368}{Ra}\right) \cdot \left(1 - \frac{2415}{Ra}\right) + \\ + 0{,}0495(Ra)^{0{,}3333} = 3{,}20,$$

$$\alpha_{cpg} = Nu\frac{\lambda}{h_{pg}} = 3{,}20\frac{0{,}0279}{0{,}03} = 2{,}98 \ \text{W/m}^2\text{·K},$$

$$\alpha_{rpg} = \varepsilon_{pg}\sigma(T_p^2 + T_g^2)(T_p + T_g) = \\ = 0{,}80 \cdot 5{,}67 \cdot 10^{-8}(333^2 + 303^2)636 = 5{,}65 \ \text{W/m}^2\text{·K},$$

$$\alpha_{g\infty} = \alpha_w + \varepsilon_g\sigma\left[0{,}25\frac{T_g^4 - T_a^4}{T_g - T_a} + 0{,}75\frac{T_g^4 - T_s^4}{T_g - T_s}\right] = \\ = 13{,}3 + 0{,}84 \cdot 5{,}67 \cdot 10^{-8} \times \\ \times \left[0{,}25\frac{303^4 - 293^4}{10} + 0{,}75\frac{303^4 - 277^4}{26}\right] = 18{,}1.$$

*Step 4 of the iteration of calculation of the air collector*

$$\lambda_f = \left[2{,}44 + 0{,}0077(T_f - 273)\right] \times 10^{-2} = \\ = \left[2{,}44 + 0{,}0077(298 - 273)\right] \times 10^{-2} = 0{,}0263,$$

$$\nu_f = (13{,}53 + 0{,}0904(T_f - 273) + \\ + 0{,}0001(298 - 273)^2) \times 10^{-6} = 15{,}85 \times 10^{-6}.$$

*Step 5 of the iteration of calculation of the air collector*

$$\text{Re}_f = \frac{\overline{\upsilon}D_h}{\nu_f} = \frac{1{,}0 \cdot 0{,}078}{15{,}85} \cdot 10^6 = 4921,$$

$$Nu_f = 0{,}0743\,\text{Re}^{0{,}76} = 4921^{.0{,}76} = 47{,}53,$$

$$\alpha_{cpf} = Nu_f\frac{\lambda}{D_h} = 47{,}53\frac{0{,}0263}{0{,}078} = 16{,}03,$$

$$\alpha_{rpb} = \varepsilon_{pb}\sigma(T_p^2 + T_b^2)(T_p + T_b) = \\ = 0{,}89 \cdot 5{,}67 \cdot 10^{-8}(333^2 + 298^2)(333 + 298) = 5{,}85.$$

*Step 6 of the iteration of calculation of the air collector*

$T_p$=321.58 K; $T_g$=307.60 K;

$T_f$=300.68 K; $T_b$=308.48 K; $T_o$=308.36 K.

*Step 7 of the iteration of calculation of the air collector*

$|T_{o1}-T_{o0}|$=|321.58–333|=11.42>0.1 proceed to step 2 with the temperatures of step 6.

*Step 8 of the iteration of calculation of the air collector*

$$U_t = \left[\frac{1}{\alpha_{cpg} + \alpha_{rpg}} + \frac{1}{\alpha_w + \alpha_{rg\infty}} + \frac{\delta_g}{\lambda_g}\right]^{-1} = \\ = \left[\frac{1}{2{,}595 + 5{,}519} + \frac{1}{18{,}073} + \frac{0{,}005}{1{,}0}\right]^{-1} = 5{,}447,$$

$$U_b = \left[\left(\frac{1}{\alpha_{cpf}} + \frac{1}{\alpha_{rpf}}\right)^{-1} + \frac{\delta_i}{\lambda_i} \cdot \frac{WL}{1 + 2WLh_f}\right]^{-1} = \\ = \left[\left(\frac{1}{16{,}08} + \frac{1}{6{,}109}\right)^{-1} + \frac{0{,}06}{0{,}04} \cdot 1{,}878\right]^{-1} = 0{,}138,$$

$U_L$=5.585;

$$F' = \frac{\alpha_{mu}}{\alpha_{mu} + U_L} = \frac{16{,}073}{16{,}073 + 5{,}585} = 0{,}742; \quad F' \cdot U_L = 4{,}144;$$

$$F_R = \frac{G_m c_p}{U_L}\left(1 - e^{-\frac{F'U_L}{G_m c_p}}\right) = \\ = \frac{0{,}06 \cdot 1005}{5{,}585}\left(1 - exp - \frac{4{,}144}{0{,}06 \cdot 1005}\right) = 0{,}717.$$

Specific heating efficiency (per 1 m² of the area of SC)

$$q_u = 0{,}717[680 - 5{,}585(296{,}91 - 293{,}0)] = 471{,}9 \ \text{W/m}^2,$$

$$\eta = \frac{471{,}9}{800} = 0{,}59.$$

The value of heating efficiency, determined through the original temperature of the flow is almost the same:

$$q_u = G_m c_p(T_o - T_a) = 0{,}06 \cdot 1005 \cdot 7{,}82 = 741{,}5 \ \text{W/m}^2.$$

Thermal power of the collector of the area of

$F = L \cdot W = 1.3 \cdot 1.7 \cdot 471.5 = 1042$ W,

$U_t = 5.515$; $U_b = 0.137$; $U_L = 5.562$;

$$F' = \frac{\alpha_h}{\alpha_h + U_L} = 0{,}743; \quad F' \cdot U_L = 4{,}133;$$

$F_R = 0.718$; $q_u = 471.3$; $\eta = 471.3/800 = 0.589$.

But if

$q_u = 0.06 \cdot 1005(28.48 - 20) = 511.3$ W,

then

$\eta = 511{,}3/800 = 0{,}639$; $\Delta\eta = 5$ %;

$U_t = 5.447$; $U_b = 0.138$; $U_L = 5.585$;

$F' = 16.08/(16.08 + 5.585) = 0.742$;

$F' \cdot U_L = 4.144$; $F_R = 0.717$;

$q_u = 471.9$; $\eta = 471.9/800 = 0.589$.

But if

$q_u = 0.06 \cdot 1005(27.82 - 20) = 471.5$,

then

$\eta = 471.5/800 = 0.589$; $\Delta\eta = 0$ %.

Thermal power of the collector with an area of

$F = L \cdot W = 1.3 \cdot 1.7 \cdot 471.9 = 1042$ W.

*The equation of the collector at small deviations of the assigned above temperature modes of heat carrier flow:*

$$q'_u = 0{,}718 \big[ 0{,}85E - 5{,}562(T_f - T_a) \big] = $$
$$= 0{,}718 \big[ 0{,}85E - 5{,}562(296{,}91 - 293) \big].$$

The lower limit of application of this equation follows from correctness of ratio (30) that is true provided that $3{,}000 < Re < 50{,}000$. Therefore, the lower limit of velocity and heat carrier flow for the channel of the height $h_f = 0.04$ m and the width $W = 1.3$ m are, respectively:

$$\overline{\upsilon}_{min} = \frac{\upsilon_f \, Re_{min}}{D_h} \approx \frac{15{,}8 \cdot 10^{-6} \cdot 3000}{0{,}078} = 0{,}061 \; \text{m/s},$$

$$G_m \geq \overline{\upsilon}_{min} h_f W \rho_n = 0{,}61 \cdot 0{,}04 \cdot 1{,}3 \cdot 1{,}2 = 0{,}038 \; \text{kg/s}.$$

At lower values of these magnitudes, the mode of the heat carrier flow transfers in the laminar, which dramatically decreases coefficient of heat transfer of the absorbing panel with a corresponding increase in the output temperature but with lower heat efficiency and efficiency coefficient.

The opposite direction of motion of the heat carrier in the inclined collector – from top to bottom – was also explored. It promotes activation of the turbulent mode at low veloc-

ities. In addition, the temperature of the incoming flow at the upper intake of the air is almost always higher compared with the ground intake due to heating the surrounding elements of the drying chamber. An increase in temperature of the outgoing flow of the heat carrier can be achieved by increasing the length of the collector and the area of the air contact with the absorption panel. In the course of such structural solutions, material consumption of the collector and energy consumption to overcome the increased resistance to the heat carrier flow decrease.

The average temperatures of the zone of the heat carrier flow at different modes of motion at the inlet of the collector and the outlet of it and the average heat transfer coefficient were found. Here, to increase the temperature of the outgoing flow, it is also necessary for decrease its consumption with the simultaneous intensification of the air flow turbulization process to retain coefficient of heat transfer and heat efficiency of the collector.

We determined the performance of the collector that is 78–80 %, which was 10–20 % higher than that of the flat collectors and 5–10 % higher than that of the cylindrical vacuumed collectors.

In conclusion, we will emphasize that the thermal balance of the collector should be considered as the method that shows the ways of arrival and losses of thermal energy taking into consideration heat efficiency at different thermo-physical parameters of the environment. This makes it possible to explore in detail the operation of the air collector and simultaneously describe the ways to improve energy efficiency of the plant and to evaluate the drying process in it when using solar energy.

## 6. Discussion of results of studying the effectiveness of operation of the air collector

The new design of the air collector with the wavy absorption plate (absorber) was developed and explored. The air collector is made in the form of a two-chamber structure separated by double glazing and a profiled metal sheet of the absorbing panel. The silicate glass of the width $W = 1.3$ m and length $L = 1.7$ m and thickness $\delta = 0.05$ m was used in the structure. The absorbing panel was made of a copper sheet of the thickness 0.5 mm with the corrugated wavy surface with the radius of rounding of 3 cm. The walls of the collector were heat-proof by the foam plastic plates of the thickness of 6 cm with coefficient of thermal conductivity $\lambda = 0.040$ W/m·K. The width and length of the back wall are accepted the same as those of the glass cover.

The methods of the step-by-step iteration of the calculation of thermo-technical characteristics of the air collector were described. In particular, we obtained theoretical dependences that make it possible to calculate the components of thermal balance and thermal equilibrium, the temperature of the heat carrier at the outlet from the collector, heating capacity and efficiency of the collector using the known geometrical dimensions of the air collector. Based on the results of theoretical research, the program for numerical computer calculation of the temperature field of heat flows was developed. This makes it possible to evaluate the influence of geometric parameters of the collector, as well as transitional modes of the motion of heat carrier on the temperature of the internal surface of the channel, coefficient of heat transfer from the wall

to the heat carrier, as well as to calculate the temperature of the heat carrier.

The average temperature zones of heat carrier flow at different modes of motion at the inlet of the collector and at the outlet from it and average heat transfer coefficient were explored. It was found that to increase the temperature of the outgoing flow of the heat carrier, it is necessary to decrease its consumption with the simultaneous intensification of the process of the air flow turbulization to retain coefficient of heat transfer and heat efficiency of the collector

During step-by-step iteration, it was found that heating efficiency of the air collector $q'_u$=471.3...511.3 W is essentially influenced by energy illuminance $E$, which is from 377 to 1,223 W/m$^2$. It was found that application of the wavy absorbing surface of the absorber in the air heliocollector at the low level of insolation $E$=377 W/m$^2$ makes it possible to increase efficiency up to η=58.3 %, and at high energy illuminance of $E$=1,000 W/m$^2$, up to η=63.9 %. This enables us to explain how re-distribution of the ratios of thermal power ($F$=1,042 W) and efficiency of the air solar collector (η=58.3–63.9 %) goes on.

Using iterative calculation, efficiency of the collector, which is more than 78–80 %, was determined, which is 10–20 % higher than that of the flat collectors and 5–10 % higher than that in the cylindrical vacuumed collectors. It was proved that theoretical dependences are adequate and can be used when calculating thermal-technical characteristics of the air collector.

Therefore, the proposed structure of the air collector by technical characteristics is not inferior to the existing solar thermal plants, specifically, flat air collectors. The use of the air collector as a part of the solar chamber for drying vegetable materials is appropriate and effective under conditions of individual farms.

The research conducted in the study is the final stage of a comprehensive research related to enhancing efficiency of the technological process of fruit drying based on the development of the design of a flat air collector. This will lead to an increase in the volume of producing high-quality dried produce with minimal power consumption due to solar energy. The results obtained will be useful for improving the technology and equipment for fruit drying.

## 7. Conclusions

1. The new design of the air collector with the air-tight warmed casing and the absorber with the wavy surface was developed, which can be used as an additional heating element of a low-temperature heat source. A number of generalizing dependences for finding heating efficiency of the collector were established, specifically, the influence of components of thermal balances of the collector on the difference of temperatures of the heat carrier flow in the collector and the level of insolation $E$ on heating efficiency $q'_u$.

2. Based on the performed research, we obtained analytical dependences for determining the components of thermal balance of the collector, distribution of temperature field along the absorbing panel, which made it possible to improve the mathematical model of the heat exchange process in the developed air collector.

3. It was found that heating efficiency of the air collector $q'_u$=471.3...511.3 W is significantly influenced by energy illuminance $E$, which is from 377 to 1,223 W/m$^2$. It was shown that the application of the wavy absorbing surface of the absorber in the air solar collector at the low level of insolation $E$=377 W/m$^2$ enables increasing efficiency up to η=58.3 %, and at high energy illuminance of $E$=1,000 W/m$^2$, up to η=63.9 %. This makes it possible to explain how re-distribution of the ratios of thermal power ($F$=1042 W) and efficiency of the air solar collector goes on.

## References

1. Parametric Study on the Thermal Performance and Optimal Design Elements of Solar Air Heater Enhanced with Jet Impingement on a Corrugated Absorber Plate / Aboghrara A. M., Alghoul M. A., Baharudin B. T. H. T., Elbreki A. M., Ammar A. A., Sopian K., Hairuddin A. A. // International Journal of Photoenergy. 2018. Vol. 2018. P. 1–21. doi: https://doi.org/10.1155/2018/1469385

2. Modelling of thermal behaviour of a direct solar drier possessing a chimney: Application to the drying of cassava / Koua K. B., Gbaha P., Koffi E. P. M., Fassinou W. F., Toure S. // Indian Journal of Science and Technology. 2011. Vol. 4, Issue 12. P. 1609–1618.

3. Distributed mathematical model supporting design and construction of solar collectors for drying / Amankwah E. A. Y., Dzisi K. A., van Straten G., van Willigenburg L. G., van Boxtel A. J. B. // Drying Technology. 2017. Vol. 35, Issue 14. P. 1675–1687. doi: https://doi.org/10.1080/07373937.2016.1269806

4. Çağlayan N., Ertekin C., Alta Z. D. Experimental investigation of various type absorber plates for solar air heaters // Journal of Agricultural Sciences. 2015. Vol. 21, Issue 4. P. 459–470.

5. Mathematical modeling of solar air collector with a trapezoidal corrugated absorber plate / Ondieki H. O., Koech R. K., Tonui J. K., Rotich S. K. // International journal of scientific & technology research. 2014. Vol. 3, Issue 8. P. 51–56.

6. Liberty J. T., Okonkwo W. I., Ngabea S. A. Solar crop drying – A viable tool for agricultural sustainability and food security // International Journal of Modern Engineering Research. 2014. Vol. 4, Issue 6. P. 8–19.

7. Theoretical and experimental investigation of the performance of back-pass solar air heaters / Alta Z. D., Çağlayan N., Atmaca İ., Ertekin C. // Turkish Journal of Engineering and Environmental Sciences. 2014. Vol. 38. P. 293–307. doi: https://doi.org/10.3906/muh-1310-2

8. Determination of emission coefficient of energyeffective glasses by calorimetric method / Burova Z. A., Dekusha L. V., Vorob'ev L. I., Mazurenko A. G. // Promyshlennaya teplotekhnika. 2011. Vol. 33, Issue 6. P. 94–100.

9. Duffie J. A., Beckman W. A. Solar Engineering of Thermal Processes. John Wiley & Sons, 2013. 910 p. doi: https://doi.org/10.1002/9781118671603

10. ASHRAE Standard 93-1986 (RA 91). Metods of Testing to Determine The Thermal Performance of Solar Collektors. Atlanta: American Society of Heating, Refrigerating and Air-Conditioning Engineers Inc., 1991.

11. ISO/FDIS 9806:2013(E). Solar energy – Solar thermal collectors – Test methods. International Organization for Standardization, 2013.

12. Yogi Goswami D. Principles of solar engineering. CRC Press, 2015. 790 p.

13. Results of research into thermal-technical characteristics of solar collector / Boyarchuk V., Korobka S., Babych M., Krygul R. // Eastern-European Journal of Enterprise Technologies. 2018. Vol. 5, Issue 8 (95). P. 23–32. doi: https://doi.org/10.15587/1729-4061.2018.142719

14. NASA Surface meteorology and Solar Energy. URL: https://eosweb.larc.nasa.gov/

Розглянуто вплив середньооб'ємної температури гілки термоелементу на основні параметри, показники надійності і динаміку функціонування термоелектричного охолоджувача при різних перепадах температури при заданому тепловому навантаженні, геометрії гілок термоелементів для характерних струмових режимів роботи. Показано, що середня температура термоелементу, яка є опорною точкою при розрахунку енергетичних показників термоелектричного охолоджувача, може бути використана тільки для розрахунків в стаціонарному режимі роботи. Використання її в динамічному режимі призводить до значних похибок. Обґрунтовано, що для динамічного режиму такою опорною точкою може служити середньооб'ємна температура термоелектричної гілки. Визначено співвідношення для оцінки среднеоб'ємної температури в залежності від відносного робочого струму. Проаналізовано зв'язки среднеоб'ємної температури термоелемента, часу виходу на стаціонарний режим, необхідну кількість термоелементів, відмінності між среднеоб'ємної і середньою температурою, холодильного коефіцієнта в залежності від відносного робочого струму. Показано, що з ростом среднеоб'ємної температури при заданому струмовому режимі роботи і перепаді температури, що перевищує 40 K, величина робочого струму, кількість термоелементів, потужність споживання, інтенсивність відмов і постійна часу зменшується, а холодильний коефіцієнт зростає. Час виходу на стаціонарний режим при переході від режиму мінімуму інтенсивності відмов в режим максимальної холодопродуктивності, знижується на 5 %, а інтенсивність відмов зростає на 16 %.

Практична значимість проведених досліджень полягає як у підвищенні якості проектування охолоджувачів, так і виборі необхідних режимів термоелектричної системи забезпечення теплових режимів електронної апаратури в залежності від значимості динамічних або критеріїв управління по надійності

Ключові слова: гілка термоелементі, середньооб'ємна температура, показники надійності, динаміка охолоджувача

# INFLUENCE OF THE MEAN VOLUMETRIC TEMPERATURE OF A THERMOELEMENT ON RELIABILITY INDICATORS AND THE DYNAMICS OF A COOLER

**V. Zaykov**
PhD, Chief of Sector
State Enterprise
«Research Institute «SHTORM»
Tereshkovoi str., 27, Odessa, Ukraine, 65076
E-mail: gradan@i.ua
**V. Mescheryakov**
Doctor of Technical Sciences, Professor,
Head of Department
Department of Informatics
Odessa State Environmental University
Lvivska str., 15, Odessa, Ukraine, 65016
E-mail: gradan@ua.fm
**Yu. Zhuravlov**
PhD, Associate Professor
Department of Technology of
Materials and Ship Repair
National University
«Odessa Maritime Academy»
Didrikhsona str., 8, Odessa, Ukraine, 65029
E-mail: ivanovich1zh@gmail.com

## 1. Introduction

When designing thermo-electric cooling devices (TED), it is necessary to take into consideration a temperature dependence of parameters for the branches of thermo-elements [1]. This circumstance is caused by the fact that the material of branches is semiconductors of different conductivity, parameters of which directly depend on temperature and the formation of temperature difference is the basic function of a thermo-electric cooler. The use of the mean temperature equal to half of the temperature difference at the ends of the thermo-element branches is possible only for a stationary mode, when temperature data are unchanged. In the dynamic mode, the mean temperature cannot serve as a reliable indicator and will lead to incorrect results of calculation of energy, dynamic and some reliability indicators of TED.

This defines the relevance of analysis into possibilities to use the mean volumetric thermo-element temperature as the